

# Scaling and universality of multipartite entanglement at criticality

Alonso Botero\*

Departamento de Física, Universidad de Los Andes, Apartado Aéreo 4976, Bogotá, Colombia and  
Department of Physics and Astronomy, University of South Carolina, Columbia, SC 29208

Benni Reznik†

Department of Physics and Astronomy, Tel Aviv University, Tel Aviv 69978, Israel.

(Dated: February 1, 2008)

Using the geometric entanglement measure, we study the scaling of multipartite entanglement in several 1D models at criticality, specifically the linear harmonic chain and the XY spin chain encompassing both the Ising and XX critical models. Our results provide convincing evidence that 1D models at criticality exhibit a universal logarithmic scaling behavior  $\sim \frac{c}{12} \log_2 \ell$  in the multipartite entanglement per region for a partition of the system into regions of size  $\ell$ , where  $c$  is the central charge of the corresponding universality class in conformal field theory.

The study of the connection between quantum entanglement and the properties of spatially extended many-body systems such as spin chains [1, 2, 3] and harmonic chains [4, 5], has recently attracted considerable attention. This connection is especially relevant for systems near, or at, certain quantum phase transitions, where well-studied features of criticality such as scale-free behavior and universality are in fact manifestations of the entanglement properties of the underlying quantum state.

Universal entanglement signatures of criticality have by now been well established in the case of pure, bipartite entanglement. Specifically, for 1D critical systems, the entanglement entropy of a region of size  $\ell$  and its complement is seen to follow the universal law  $S \sim \frac{c}{3} \log_2 \ell$ , where  $c$  is the central charge characterizing a corresponding universality class in conformal field theory (CFT) in the continuum limit. First obtained for continuous fields within the CFT framework [6], the result has by now been widely verified in discrete systems such as spin chains [7], harmonic chains [5], and fermions [8, 9].

That many-body systems should also manifest properties of genuine multipartite entanglement (MPE) has been evidenced, for example, in spin chains [10, 11, 12, 13], and as shown in the simulation of many-body ground states within the matrix-product state framework [14], MPE at criticality may be highly non-trivial. Connections between critical behavior and MPE in 1D spin models have been particularly elaborated by [15, 16, 17, 18], which find non-analytic behavior of MPE at criticality and other signs of universality.

In this Letter we further explore the MPE of critical 1D systems by addressing a question in the spirit of renormalization that naturally arises in this context: Given the scale-free nature of the continuum limit of the critical system, how does the MPE between regions of the same size scale under coarse- or fine-graining, that is, as we vary the size of the regions (Fig. 1)? We investigate this problem in both harmonic and XY spin chains, using as a measure of MPE the geometric measure of Wei and

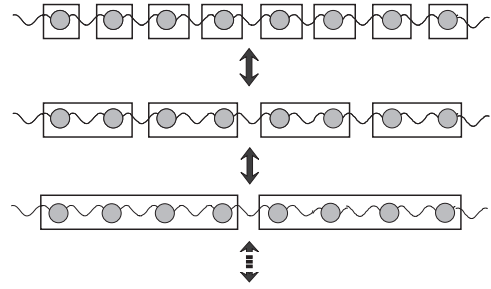


FIG. 1: Coarse graining of a system to  $N$  regions of size  $\ell$ , with  $Nl$  fixed.

Goldbart [15, 19]. Our main finding is that with respect to a partition of the system into equal regions of size  $\ell$ , the geometric MPE per region,  $\mathcal{E}$ , shows the logarithmic scaling behavior

$$\mathcal{E} \sim \frac{c^*}{12} \log_2 \ell \quad (1)$$

at criticality. Here,  $c^*$  is a constant that most probably is the central charge of the relevant universality class, as evidenced from our numerical results and the correspondence with the case bipartite case, for which a connection can be established independently using previous results in the literature.

For an entangled state of  $N$  parties, the geometric entanglement measure [19] is defined as  $E(\psi) = -\log |\Lambda|^2$ , where  $|\Lambda|^2$  is the maximal overlap  $|\langle \psi | \phi_1 \phi_2 \dots \phi_N \rangle|^2$  over all possible product states  $|\phi_1 \phi_2 \dots \phi_N\rangle$ ; the optimal states and  $\Lambda$  are in turn solutions to the nonlinear eigenvalue equation

$$\langle \phi_1 \phi_2 \dots \hat{\phi}_i \dots \phi_N | \psi \rangle = \Lambda |\phi_i\rangle, \quad (2)$$

where  $\hat{\phi}_i$  stands for the exclusion of the state  $|\phi_i\rangle$ . Here, we will be interested in the ground state  $|\psi\rangle$  of large circular chains of spins and oscillators, with the  $N$  parties representing regions of size  $\ell$  each, so that the total

number of spins or oscillators is  $N\ell$ . Considerable simplifications of the nonlinear eigenvalue problem under these conditions allow for a feasible numerical implementation of the solution: First, due to translational invariance, the optimal state takes the form  $|\phi\rangle^{\otimes N}$ , and the problem reduces to finding a single state  $|\phi\rangle$  for one region. Furthermore, ground states of oscillator and spin chains in the XY model are both describable in the language of bosonic or fermionic gaussian states, where the connection in the XY case is through a Jordan-Wigner transformation to effective fermion variables. Since partial tracing is a gaussian operation, a solution to Eq. (2) can be found within the class of gaussian states. As is well known, gaussian states can be characterized by a single covariance matrix[20] that takes the block form

$$\mathbf{M}_{\text{boson}} = \begin{pmatrix} \mathbf{G} & \mathbf{K} \\ \mathbf{K}^T & \mathbf{H} \end{pmatrix}, \quad \mathbf{M}_{\text{fermion}} = \begin{pmatrix} \mathbf{A} & \mathbf{C} \\ -\mathbf{C}^T & \mathbf{B} \end{pmatrix}, \quad (3)$$

where  $\mathbf{M}_{\text{boson}}$  is symmetric and  $\mathbf{M}_{\text{fermion}}$  is antisymmetric. Further simplification follows from the fact that in the cases of interest, the conditions  $\mathbf{K} = 0$  and  $\mathbf{A} = \mathbf{B} = 0$  are satisfied. For pure states, these conditions imply that in the bosonic case  $\mathbf{G}\mathbf{H} = \mathbb{1}$ , while in the fermionic case  $\mathbf{C}\mathbf{C}^T = \mathbb{1}$ ; thus, all the information of the gaussian state can be encoded in a single block (e.g.,  $\mathbf{G}$  or  $\mathbf{C}$ ). We shall therefore refer to a single  $N\ell \times N\ell$  matrix  $\boldsymbol{\Omega}$  for the full state  $|\psi\rangle$  and an  $\ell \times \ell$  matrix  $\boldsymbol{\omega}_{\text{opt}}$  for the optimal state  $|\phi\rangle$ , where both  $\boldsymbol{\Omega}$  and  $\boldsymbol{\omega}$  are either symmetric (bosonic) or orthogonal (fermionic). Finally, due to translational symmetry,  $\boldsymbol{\Omega}$  has a Toeplitz form at the level of  $\ell \times \ell$  blocks, and may thus be brought through a matrix version of Bloch's theorem to the block-diagonal form  $\boldsymbol{\omega} = \bigoplus_{\eta} \boldsymbol{\omega}_{\eta}$  where the set  $\{e^{i\eta}\}$  are the  $N$ th roots of unity, and the  $\boldsymbol{\omega}_{\eta}$  are hermitian (bosonic) or unitary (fermionic)  $\ell \times \ell$  matrices, given by

$$[\boldsymbol{\omega}_{\eta}]_{ij} = \frac{1}{N} \sum_{m=0}^{N-1} [\boldsymbol{\Omega}]_{m\ell+i, j} e^{im\eta}. \quad (4)$$

The optimal gaussian solution to the eigenvalue problem of Eq. 2 can then be recast as the equation

$$\boldsymbol{\omega}_{\text{op}}^{-1} = \frac{1}{N} \sum_{\eta} \frac{2}{\boldsymbol{\omega}_{\text{op}} + \boldsymbol{\omega}_{\eta}}. \quad (5)$$

With this form, a numerical computation of  $\boldsymbol{\omega}_{\text{opt}}$  can be obtained iteratively starting with a trial  $\boldsymbol{\omega}_{\text{opt}}$  in the right hand side and iterating until a fixed point is reached. Our experience shows that in most cases twenty or so iterations suffice to reach an acceptable fixed point.

Once  $\boldsymbol{\omega}_{\text{opt}}$  is determined, the geometric entanglement can be obtained from the sum  $E(\psi) = \sum_{\eta} E_{\eta}$ , where

$$E_{\eta}(\psi) = \pm \log_2 \left| \frac{\det \frac{1}{2} [\boldsymbol{\omega}_{\text{op}} + \boldsymbol{\omega}_{\eta}]}{\sqrt{\det \boldsymbol{\omega}_{\text{op}} \det \boldsymbol{\omega}_{\eta}}} \right|, \quad (6)$$

are the partial contributions from each sector and where the minus sign applies to the fermionic case. The average of the partial entanglements  $E_{\eta}(\psi)$  gives the entanglement per region or *entanglement density*  $\mathcal{E}(\psi) \equiv E(\psi)/N$ , which is our quantity of interest.

We first consider the circular harmonic chain described by a Hamiltonian with a single parameter  $0 \leq \alpha < 1$ ,  $H_{\alpha} = \sum \frac{p_i^2}{2} + \frac{q_i^2}{2} - \alpha q_i q_{i+1}$ , with  $i$  periodic in  $N\ell$ . Here,  $\boldsymbol{\Omega}$  has entries given by  $[\boldsymbol{\Omega}]_{ij} = 2g(|i - j|)$  where  $g(l)$  is the momentum correlation function  $\langle p_0 p_l \rangle$  and is diagonalized by discrete circular wave normal mode functions indexed by an angle  $\theta_k = \frac{2\pi}{N\ell}k$ , with eigenvalues given by the dispersion relation  $\omega(\theta_k) = \sqrt{1 - \alpha \cos(\theta_k)}$ . For finite  $\alpha$ , the correlation function decays exponentially with  $l$  with correlation length  $\xi \simeq 1/\sqrt{2(1 - \alpha)}$ . Criticality corresponds to the limit  $\alpha \rightarrow 1$ , in which the system becomes gapless, ( $\omega(\theta) \propto |\theta|$  for small theta), the correlation length diverges, and the correlation function exhibits power-law behavior  $g(l) \sim 1/l^2$ .

It will be instructive to briefly develop a picture of the optimal solution based on the Bloch decomposition of  $\boldsymbol{\Omega}$ . In the harmonic chain, the  $\boldsymbol{\omega}_{\eta}$  are given in terms of the dispersion relation  $\omega(\theta)$  and circular plane waves with shifted node numbers

$$[\boldsymbol{\omega}_{\eta}]_{ij} = \frac{1}{\ell} \sum_{k=0}^{\ell-1} \omega(\theta_{k+\nu_{\eta}}) e^{i\theta_{k+\nu_{\eta}}(i-j)} \quad (7)$$

where  $\nu_{\eta} = (\eta \bmod 2\pi)/2\pi$  is the winding number of  $\eta$ . We can interpret  $\boldsymbol{\omega}_{\eta}$  as (twice) the momentum correlation matrix  $\langle \pi_i \pi_j^{\dagger} \rangle_{\eta}$  for the vacuum state of a complex scalar field on a linear lattice of  $\ell$  points, with Hamiltonian  $H_{\eta} = \frac{1}{2}\pi^{\dagger} \cdot \pi + \frac{1}{2}\phi^{\dagger} \mathbf{V}_{\eta} \phi$  and potential matrix  $\mathbf{V}_{\eta} = \boldsymbol{\omega}_{\eta}^2$ , where

$$[\mathbf{V}_{\eta}]_{ij} = \delta_{ij} + \frac{\alpha}{2} [\delta_{|i-j|,1} + e^{i\eta} \delta_{i,1} \delta_{j,\ell} + e^{-i\eta} \delta_{i,\ell} \delta_{j,1}] \quad (8)$$

(this result is easily derived by applying the Bloch decomposition to the potential matrix for the whole chain). The case  $\eta = 0$  corresponds to a translationally invariant closed chain of  $\ell$  oscillators, while for  $\eta \bmod 2\pi \neq 0$ , translational invariance is lost by the appearance of a “twisted” coupling between the first and last oscillators, which in the continuum correspond to the twisted boundary conditions  $\phi(0) = e^{i\eta}\phi(\ell)$  for a complex Klein-Gordon field. Now, due to periodicity in  $\eta$ , the  $\boldsymbol{\omega}_{\eta}$  describe a closed loop in the space of Hermitian  $\ell \times \ell$  matrices, and  $\boldsymbol{\omega}_{\text{op}}$  corresponds to a generalized “center of mass” for this loop with respect to the distance measure (6). As  $\ell$  becomes large, the perturbation to the free modes on the circular chain becomes noticeable only at the longest wavelengths, for which  $\delta\lambda/\lambda = \nu/k$  is appreciable, and gives rise to small  $\sim 1/\ell$  corrections to the spectrum. Thus we expect that the distances  $E_{\eta}$  should converge to a common value for large  $\ell$ . However, it is important to note that as  $\alpha \rightarrow 1$ , the partial contribution  $E_{\eta=0}$  diverges independently of  $\boldsymbol{\omega}_{\text{opt}}$ , this is due to

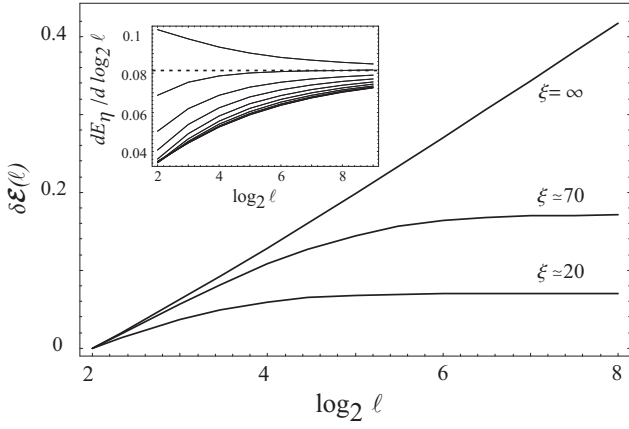


FIG. 2: Block size dependence of the geometric entanglement per block  $\mathcal{E} = E/N$ , as measured from its value at  $\ell = 4$  ( $\delta\mathcal{E}(\ell) \equiv \mathcal{E}(\ell) - \mathcal{E}(4)$ ) vs.  $\log_2 \ell$ , for three values of the correlation length  $\xi$  in the harmonic chain, for  $N = 10$  blocks. Inset: Convergence of the slopes of partial contributions  $E_\eta$  as function of  $\log_2 \ell$ , for  $N = 20$ , at criticality. Curve order (starting from bottom curve) proportional to  $|\eta - \pi|$  with  $\eta \in [0, 2\pi)$ ; dashed line corresponds to  $c/12 \simeq 0.0833$ .

the vanishing determinant of  $\omega_{\eta=0}$  and in turn to the dispersion relation  $\omega(\theta) = 0$  for the  $\theta = 0$  mode at criticality. Thus, for  $\eta = 0$ , the relevant distance as  $\alpha \rightarrow 1$  should in fact be taken to be  $E_{\eta=0}^{(ren)} = E_{\eta=0} - E_{\text{div}}$ , where  $E_{\text{div}} \equiv -\frac{1}{2} \log \omega(0) \simeq \frac{1}{2} \log_2 \xi$  is the divergent contribution of the zero mode. The renormalized distances are well-defined at criticality and are indeed seen to converge to common values as  $\ell \rightarrow \infty$ .

Turning now to our numerical results, we first note that the use of an entanglement density is indeed appropriate, as the (renormalized) densities rapidly converge to  $N$ -independent values at small values of  $N$ . This can be attributed to the fact that increasing the density of points in the previously mentioned closed loop of hermitian matrices, has only minor effects on the location of the “center of mass”. We also comment on the optimum matrix  $\omega_{op}$ : the corresponding potential matrix  $V_{op} = \omega_{op}^2$  was found to have, up to small fluctuations, the same structure of that of a chain of length  $\ell$  with the same value of  $\alpha$  but with open boundary conditions; thus, in a first approximation, the optimum potential matrix appears to be the average of the  $V_\eta$  matrices as one may expect from the center of mass picture. Turning then to the entanglement density as a function of  $\ell$ , in Fig. 2 we present our results for different correlation lengths  $\xi$ . As can be seen, the increase in entanglement for non-critical values saturates when  $\ell \sim \xi$ . This limiting behavior can be attributed to the entanglement of oscillators within a distance  $\sim \xi$  from the interfaces between regions, in which case the total entanglement is determined only by the number of partitions. On the other hand, at criticality  $\xi = \infty$ , the renormalized entanglement per region is

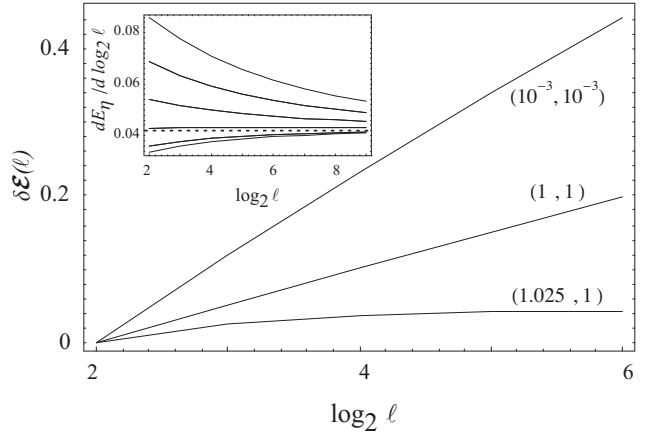


FIG. 3: Block size dependence of the geometric entanglement per block  $\mathcal{E} = E/N$ , as measured from its value at  $\ell = 4$  ( $\delta\mathcal{E}(\ell) \equiv \mathcal{E}(\ell) - \mathcal{E}(4)$ ) vs.  $\log_2 \ell$ , for three values of  $(\gamma, \lambda)$  on the phase plane in the  $XY$  model, for  $N = 20$  blocks. From top to bottom: vicinity of the bosonic critical line ( $XX$  model), fermionic critical line (Ising), and a non critical value showing saturation. Inset: Convergence of the partial contributions  $E_\eta$  as function of  $\log_2 \ell$ , for  $N = 10$ , at the Ising model critical point. Curve heights follow same order as in Fig; dashed line corresponds to  $c/12 \simeq 0.0417$ .

found to scale with  $\ell$  as

$$\mathcal{E}^{(ren)}(\psi) = \kappa^* \log_2 \ell \quad (9)$$

where  $\kappa^*$  is a coefficient that one may expect to depend on the CFT central charge  $c = 1$ , as does the bipartite entanglement entropy. For the finite values considered in our computations, the coefficient  $\kappa^*$  in fact varies slowly as  $\ell$  is increased and it therefore becomes difficult to infer the limiting value from the total entanglement density. However, an examination of the instant slopes of the partial contributions  $E_\eta$  reveals (as shown in Fig. 2) that they all converge to a single limiting value, from both directions. We have estimated this limiting value by fitting the instantaneous slopes to the function  $\kappa_\nu(\ell) = \kappa^* + A(\nu)\ell^{-\lambda}$ , where  $A(\nu)$  is quadratic in  $\nu$  and symmetric about  $\nu = 1/2$  (from periodicity), for various values of partitions up to  $N = 100$ , and obtain that  $\kappa^* = 0.0837$  with a 5% error, independently of the number  $N$  of partitions. Within the margin of error, this value is consistent with  $\kappa^* = c/12$  where  $c$  is the central charge  $c = 1$  of the bosonic CFT universality class.

To test the universality of our results, we consider the  $XY$  spin chain model, which includes two critical regions associated with different CFT universality classes. The  $XY$  Hamiltonian takes the form  $H_{\lambda,\gamma} = -\sum \lambda Z_i + \frac{1+\gamma}{2} X_i X_{i+1} + \frac{1-\gamma}{2} Y_i Y_{i+1}$ , where  $X_i, Y_i, Z_i$  are Pauli matrices at the site  $i$ , and the anisotropy  $\gamma$  and the field strength  $\lambda$  parametrize the ground state phase diagram. The critical lines are  $\gamma = 0$ , associated with the bosonic ( $c = 1$ ) universality class, and  $\lambda = 1$ , as

sociated with the fermionic ( $c = 1/2$ ) class. By means of a Jordan-Wigner transformation,  $H_{\lambda,\gamma}$  can be transformed to a free fermions system, the ground state of which is gaussian fermionic and can be characterized by an orthogonal matrix  $\Omega$  with eigenvalues

$$\omega(\theta) = \frac{(\cos(\theta) - \lambda) - i\gamma \sin(\theta)}{\sqrt{(\cos(\theta) - \lambda)^2 + \gamma^2 \sin(\theta)}} \quad (10)$$

and circular plane waves with momentum label  $\theta$  as eigenstates. The corresponding  $\omega_\eta$  matrices can be obtained by using this expression for  $\omega(\theta)$  in Equation 7.

As depicted in Figure 3, the XY model also shows saturation for non- critical regions and logarithmic scaling behavior for spin chain models in at criticality. For the critical Ising point,  $\gamma = \lambda = 1$ , very good agreement is obtained with  $\kappa^* \sim 0.043$ , consistent with  $c/12$  for  $c = 1/2$ . In the critical  $XX$  case,  $\lambda = 0$ ,  $0 \leq \gamma < 1$ , our iteration scheme converges slower, and large  $\ell$  values become harder to obtain numerically due to precision losses at every iteration. Still, logarithmic scaling was evidenced with  $\kappa^*$  consistent with  $c/12$  for  $c = 1$  within 15%.

The slope value  $c/12$  is consistent with the results for  $N = 2$ , which are analytically tractable, owing to the fact that in the bipartite case the geometric entanglement is the logarithm of the largest Schmidt coefficient of the state. As discussed in [21, 22], with respect to any bi-partite split the ground state of a quadratic boson or fermion hamiltonian can always be expressed as the product of two-mode entangled states of the form  $(1 \pm e^{-\beta})^{\pm 1/2} \sum_n e^{-\beta n} |n, n\rangle$  where the  $\beta$ 's are related to the symplectic eigenvalues of the reduced covariance matrix and  $n$  goes from zero to  $\infty$  for bosons, or 1 for fermions. The geometric entanglement is therefore the “free energy”  $E = \pm \sum_\beta \log(1 \pm e^{-\beta})$  coming from the  $n = 0$  coefficients. In the continuum limit this quantity is equal to half the von Neumann entropy, if the density of modes is constant for the range of contributing modes  $\beta \lesssim 1$ , as occurs at criticality (a rigorous derivation is found in [23]). Using the result of Calabrese and Cardy [24], where for a symmetric split of a chain of size  $2\ell$ , the entanglement entropy is found to scale like  $S \sim \frac{c}{3} \log \ell$ , the resulting geometric entanglement density is then found to be  $\mathcal{E}_{N=2} = \frac{1}{2}E = \frac{1}{4}S$ , and thus to scale as  $\sim \frac{c}{12} \log \ell$ .

Elsewhere, Bravyi[25] has proposed a generalization of the entanglement entropy for multipartite states, corresponding to the minimum attainable Shannon entropy of the joint measurement outcome distribution when considering all possible multilocal measurement bases. Since the overlap between an entangled state  $|\psi\rangle$  and any product state cannot exceed in magnitude the maximal value  $|\Lambda|$  from eq. (2), the Shannon entropy of the squares of the coefficients in any product basis expansion of the state cannot exceed the entropy  $-\log_2 |\Lambda|^2$  of an equally-weighted superposition of  $1/|\Lambda|^2$  product-state terms. The geometric entropy is therefore a lower bound on the

multipartite entanglement entropy. Roughly speaking, such an entropy may be considered a measure of the effective Schmidt number [26], or number of terms in a multilocal orthogonal decomposition of the state. Our result therefore suggests that at criticality this effective number must scale with the region size  $\ell$  no slower than  $\sim \ell^{\frac{N_c}{12}}$ . An interesting open question is the extent to which the exponent  $\frac{N_c}{12}$  is a good characterization of the actual effective Schmidt number of 1D ground states for critical systems.

To conclude, in the present work we found convincing evidence that multi-partite entanglement in 1D systems, manifests at criticality a logarithmic scaling behavior as well as universality; properties which have so far been established only for bi-partite entanglement at criticality. This finding, has been here demonstrated for free Gaussian harmonic and spin chain models, and will hopefully be further tested in other discrete solvable models, as well as in the framework of conformal field theory. It would be also very interesting to formulate the problem at hand in conformal field theory, since the connection of the present result with some properties of CFT is at present an intriguing open question. Finally we hope that, the emerging understanding of the properties and structure of entanglement in many-body systems, will also turn helpful in further developing tools for studying many-body systems.

A.B. acknowledges support from Colciencias, contract RC-2005-2003, B.R. acknowledges the Israel Science Foundation, grant 784/06.

---

\* Electronic address: abotero@uniandes.edu.co

† Electronic address: reznik@post.tau.ac.il

- [1] K. M. O’Connor, W. K. Wootters , Phys. Rev. A **63** (2001) 052302
- [2] T. J. Osborne and M. A. Nielsen, Phys. Rev. A **66**, 032110 (2002).
- [3] A. Osterloh, L. Amico, G. Falci, and R. Fazio, Nature **416**, 608 (2002).
- [4] K. Audenaert, J. Eisert, M.B. Plenio, R.F. Werner, Phys. Rev. A **66**, 042327 (2002)
- [5] A. Botero and B. Reznik, Phys. Rev. A **70**, 052329 (2004).
- [6] C. Holzhey, F. Larsen, and F. Wilczek, Nucl. Phys. B **300**, 377 (1994).
- [7] G. Vidal, J. I. Latorre, E. Rico, and A. Kitaev, Phys. Rev. Lett. **90**, 227902 (2003).
- [8] M. M. Wolf, Phys. Rev. Lett. **96**, 010404 (2006).
- [9] D. Gioev and I. Klich, Phys. Rev. Lett. **96**, 100503 (2006).
- [10] D. Bruss, N. Datta, A. Ekert, L. C. Kwek, and C. Macchiavello, PRA **72**, 014301 (2005).
- [11] A. Lakshminarayanan and V. Subrahmanyam, Phys. Rev. A **71**, 062334 (2005).
- [12] R. Somma *et. al.*, Phys. Rev. A **70**, 042311 (2004).
- [13] G. Costantini *et. al.*, J. Phys. A: Math. Theor. **40**, 8009

(2007).

[14] D. Perez-Garcia, F. Verstraete, M.M. Wolf, J.I. Cirac, *Quantum Inf. Comput.* **7**, 401 (2007).

[15] T. C. Wei, D. Das, S. Mukhopadhyay, S. Vishveshwara, and P. M. Goldbart, *Phys. Rev. A* **71**, 060305(R) (2005).

[16] Han-Dong Chen, *J. Phys. A: Math. Theor.* **40**, 10215 (2007).

[17] T. R. de Oliveira, G. Rigolin, M. C. de Oliveira, *Phys. Rev. A* **73**, 010305(R) (2006).

[18] T. R. de Oliveira *et. al.* *Phys. Rev. Lett.* **97**, 170401 (2006).

[19] T. C. Wei and P. M. Goldbart, *Phys. Rev. A* **68**, 042307 (2003).

[20] In terms of  $x_i = a_i + a_i^\dagger$ ,  $y_i = i(a_i^\dagger - a_i)$  for fermions, and  $x_i = (a_i + a_i^\dagger)/\sqrt{2}$ ,  $y_i = (a_i - a_i^\dagger)/\sqrt{2}i$  for bosons, and  $\eta = (x_1, x_2, \dots, y_1, y_2, \dots)$  we have  $[M_{\text{fermion}}]_{\alpha, \beta} = \frac{1}{2i} \langle [\eta_\alpha, \eta_\beta] \rangle$  and  $[M_{\text{boson}}]_{\alpha, \beta} = \frac{1}{2} \langle \{\eta_\alpha, \eta_\beta\} \rangle$ .

[21] A. Botero and B. Reznik, *Phys. Rev. A* **67**, 52311 (2003).

[22] A. Botero and B. Reznik, *Phys. Lett. A* **331**, 39 (2004).

[23] R. Orús, J. I. Latorre, J. Eisert, and M. Cramer, *Phys. Rev. A* **73**, 060303(R) (2006).

[24] P. Calabrese and J. Cardy, *J. of Stat. Mech.* **0406**, 002 (2004).

[25] S. Bravyi, *Phys. Rev. A* **67**, 012313 (2003).

[26] J. Eisert and H. J. Briegel, *Phys. Rev. A* **64**, 022306 (2001)